The Astrophysical Journal, 660:1480–1485, 2007 May 10

PISMIS 24-1: THE STELLAR UPPER MASS LIMIT PRESERVED[1]

J. Maíz Apellániz[2]
Instituto de Astrofísica de Andalucía-CSIC, 18008 Granada, Spain; jmaiz@iaa.es

Nolan R. Walborn
Space Telescope Science Institute, Baltimore, MD 21218

N. I. Morrell
Las Campanas Observatory, Observatories of the Carnegie Institution of Washington, La Serena, Chile

V. S. Niemela[3,4]
Facultad de Ciencias Astronómicas y Geofísicas, Universidad Nacional de La Plata, 1900 La Plata, Argentina

AND

E. P. Nelan
Space Telescope Science Institute, Baltimore, MD 21218
Received 2006 December 1; accepted 2007 January 19

ABSTRACT

Is there a stellar upper mass limit? Recent statistical work seems to indicate that there is and that it is in the vicinity of 150 $M_{\odot}$. In this paper we use *HST* and ground-based data to investigate the brightest members of the cluster Pismis 24, one of which (Pismis 24-1) was previously inferred to have a mass greater than 200 $M_{\odot}$, in apparent disagreement with that limit. We determine that Pismis 24-1 is composed of at least three objects, the resolved Pismis 24-1SW and the unresolved spectroscopic binary Pismis 24-1NE. The evolutionary zero-age masses of Pismis 24-1SW, the unresolved system Pismis 24-1NE, and the nearby star Pismis 24-17 are all $\approx$100 $M_{\odot}$, very large but under the stellar upper mass limit.

Subject headings: binaries: close — stars: early-type — stars: fundamental parameters — stars: individual (Pismis 24-17, Pismis 24-1NW, Pismis 24-1SE)

1. INTRODUCTION

Massive stars strongly influence the structure and evolution of galaxies; thus, accurate knowledge of their fundamental parameters is critical. The spectroscopic binary frequency alone for OB stars is near 50%; moreover, they are preferentially formed in compact multiple systems (Mason et al. 1998). Multiplicity therefore introduces a basic uncertainty in the determination of OB-star parameters, and it must be established with the greatest precision. Radial velocities are sensitive to separations up to a few AU; larger separations must be detected by means of high angular resolution. Even in the near solar neighborhood, barely resolved or unresolved OB multiple systems are known (Walborn et al. 1999; Nelan et al. 2004 and references therein). The unobservable gap in separations of course increases with distance, but it will be reduced with more powerful instruments.

One important desideratum is the stellar upper mass limit. The O3 (Walborn 1971) and O2 (Walborn et al. 2002, hereafter W02) spectral types include some of the most massive stars known. However, it is essential to know their multiplicities in order to determine their actual masses and solve the existing discrepancy between the highest accurate mass measured spectroscopically (83 $M_{\odot}$; Rauw et al. 2004; Bonanos et al. 2004) and the photometric masses in the range 120–200 $M_{\odot}$ found by several authors. Another important desideratum is knowing how multiplicity influences the calculation of the initial mass function (IMF) at its high-mass end. Unresolved multiple systems artificially flatten the IMF by shifting objects from lower mass bins into higher mass ones. A sign of that effect is the change in the $\log M - \log L$ slope in the empirical relation derived from binary systems (Niemela & Gamen 2004). At first glance, the Magellanic Clouds would appear to be the ideal place to study the flattening of the IMF, given their low extinction and foreground contamination and the small contribution of depth effects. However, the very massive stars there are located typically an order of magnitude farther away than their Galactic counterparts; hence, for the Magellanic Clouds we are even more limited by the angular resolution of our instruments.

Several authors (Weidner & Kroupa 2004; Figer 2005; Oey & Clarke 2005; Koen 2006) have recently used the observed distribution of stellar masses in R136 and other young clusters and associations to establish that either (1) a stellar upper mass limit of $\sim$150 $M_{\odot}$ exists or (2) the IMF becomes much steeper beyond 100 $M_{\odot}$. However, when W02 analyzed the earliest O-type stars known, they found two apparent exceptions to that limit, the most egregious being Pismis 24-1 (also known as HDE 319718A and LSS 4142A). Two different mass estimates for that star, based on the evolutionary calibration of Vacca et al. (1996) and on the models by Schaller et al. (1992) yield 291 and 210 $M_{\odot}$, respectively. Pismis 24-1 was classified as an O4 (f) star by Lortet et al. (1984), as O3 III by Vijapurkar & Drilling (1993), as O3 If* by Massey

[1] This article is based on data gathered with three facilities: the NASA/ESA *Hubble Space Telescope* (*HST*), the 6.5 m Magellan Telescopes at Las Campanas Observatory (LCO), and the 2.15 m J. Sahade telescope at Complejo Astronómico El Leoncito (CASLEO). The *HST* observations are associated with GO program 10602. *HST* is controlled from the Space Telescope Science Institute, which is operated by the Association of Universities for Research in Astronomy, Inc., under NASA contract NAS 5-26555. CASLEO is operated under agreement between CONICET, SeCyT, and the Universities of La Plata, Córdoba and San Juan, Argentina.

[2] Ramón y Cajal fellow.

[3] Member of Carrera del Investigador, CIC-BA, Argentina.

[4] Deceased.

et al. (2001), and as O3.5 If* by W02. Another star in the same cluster, Pismis 24-17 (also known as HDE 319718B), which also appears to be very massive (101 $M_\odot$ according to W02), was classified as O3–4 V by Lortet et al. (1984), as O3 III(f*) by Massey et al. (2001), and as O3.5 III(f*) by W02. Both objects were recently shown by Morrell et al. (2005) to have the same O IV and N IV features in the 3400 Å region as other stars with similar spectral classifications, thus confirming their spectral types. Pismis 24-1 and 24-17 are the main sources of ionizing photons for the H II region G353.2+0.9 in NGC 6357 (Bohigas et al. 2004).

In this paper we present new observations that resolve the discrepancy between the $\sim$150 $M_\odot$ stellar upper mass limit found in clusters and the larger apparent mass of Pismis 24-1.

2. DATA

2.1. *Imaging*

In order to study the multiplicity at the high-mass end of the IMF, we were granted *HST* time in GO program 10602. The sample was drawn from an updated version of the Galactic O star catalog (Maíz Apellániz et al. 2004) by choosing all stars with spectral types O3.5 and earlier. A total of 20 objects with previous spectral classifications as O2–3.5 in 12 fields were observed with ACS WFC (the Wide Field Channel of the Advanced Camera for Surveys) in F435W+F550M+F850LP and with ACS HRC (the High Resolution Channel of the same instrument) in a variety of filters (one of the objects had already been observed in another of our programs, GO 10205). The Pismis 24 field was observed on 2006 April 5 using the above mentioned filters for the WFC and F220W+F250W+F330W+F435W+F550M+F658N+F850LP for the HRC (Fig. 1). The HRC data were centered on the core of Pismis 24 and were dithered using two- or four-point patterns, depending on the filter. The individual HRC exposure times were selected to maximize S/N in all filters for the brightest stars while avoiding saturation. The resulting total integration times ranged from 2 s (F850LP) to 704 s (F220W). The WFC data cover a large fraction of the cluster and were dithered using a two-point pattern. The WFC exposures had total integration times of 460–678 s for each of the three filters. No short WFC exposures could be added due to the large overheads involved; hence, the bright stars were heavily saturated, as evidenced by the obvious bleeding in the top panel of Figure 1.

The ACS HRC is an excellent detector for high-resolution imaging, with a pixel size of $\approx$0.028″ (the exact value depends on the position), a well-characterized PSF, and a very precise geometric distortion solution (Anderson & King 2004; Maíz Apellániz 2007a). Those properties allowed us to easily resolve Pismis 24-1 into two components of similar brightness (see bottom panel of Fig. 1) in all of the seven HRC filters.[5] Given the similar magnitudes of the two components (see below), we will use the notation Pismis 24-1NE and Pismis 24-1SW in order to avoid possible confusion. Pismis 24-17, on the other hand, appears to be unresolved in all of the HRC filters, with its profile being essentially indistinguishable (apart from S/N effects) from that of the other bright isolated star in the HRC field.

One of us (J. M. A.) has recently written a crowded-field photometry package, JMAPHOT, especially tailored for the *HST* instruments. For ACS, the code utilizes the SCI_COR (scientific, corrected) files which are the result of applying `multidrizzle`

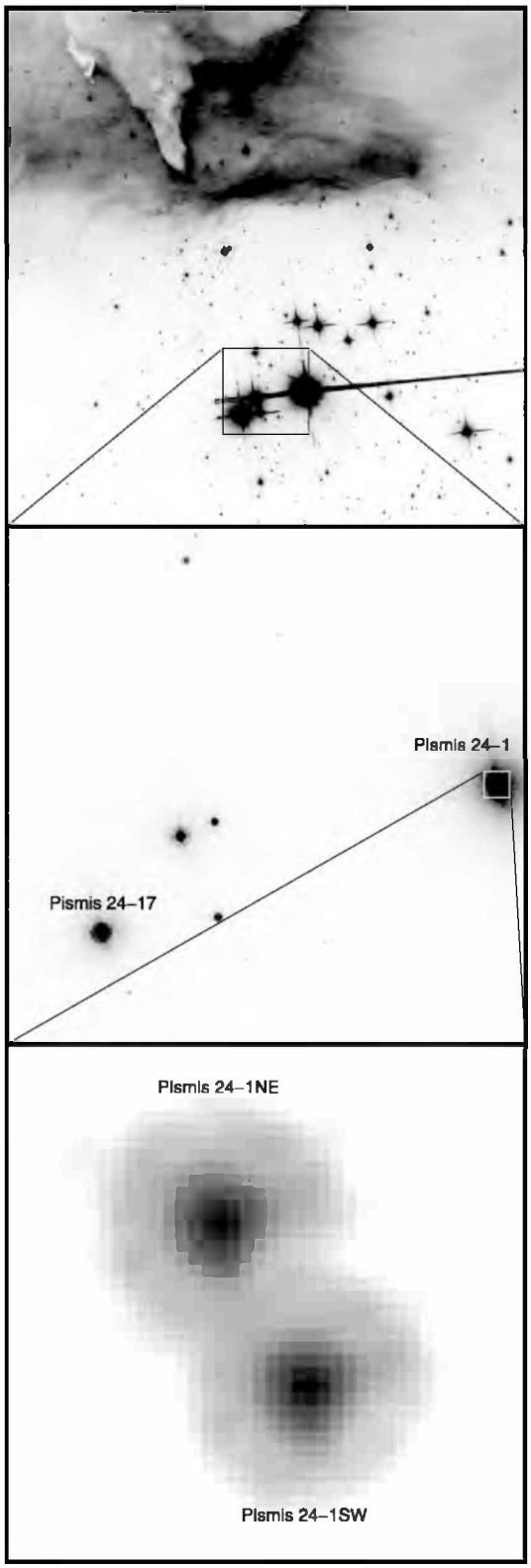

FIG. 1.—*HST* ACS imaging of Pismis 24. *Top*: The 2′ × 2′ FOV from the WFC F850LP drizzled data. *Middle*: The 20″ × 20″ FOV from the HRC F850LP drizzled data. *Bottom*: The 1″ × 1″ FOV from the HRC F435W drizzled data. In all cases north is toward the top and east toward the left. In the top and middle panels the intensity scale is linear, while in the bottom one a logarithmic scale was selected to highlight the PSF. The bright stars in the top panel are heavily saturated.

[5] The WFC, with a pixel size approximately double that of the HRC, can also resolve the system. The strong saturation prevents this from being immediately obvious in the top panel of Fig. 1. However, a closer inspection of the bleeding trail that originates from Pismis 24-1 reveals that it is double.

TABLE 1
ACS HRC Photometry Expressed in VEGAMAG

Object	F220W	F250W	F330W	F435W	F550M	F658N	F850LP
Pismis 24-1NE	16.628 ± 0.051	14.513 ± 0.051	13.103 ± 0.010	12.781 ± 0.006	10.996 ± 0.017	9.846 ± 0.005	8.360 ± 0.050
Pismis 24-1SW	16.741 ± 0.051	14.621 ± 0.051	13.202 ± 0.010	12.897 ± 0.006	11.111 ± 0.017	10.030 ± 0.005	8.510 ± 0.050
Pismis 24-17	17.504 ± 0.051	15.451 ± 0.051	14.027 ± 0.012	13.654 ± 0.006	11.783 ± 0.023	10.640 ± 0.004	9.011 ± 0.050

to the FLT (flat-fielded) files in order to produce a DRZ (drizzled) frame. The SCI_COR files have the advantages of being free of cosmic rays and hot pixels and, at the same time, having the same geometric properties of the FLT files. Using geometrically uncorrected data allows for more precise position measurements and does not modify the photon statistics (i.e., adjacent pixels do not have correlated errors), thus improving the reliability of PSF fitting (Anderson & King 2004). On the other hand, working on a geometrically distorted frame introduces some inconveniences, such as making the calculation of positions and aperture corrections less straightforward. When bright isolated stars are present, as is the case for our Pismis 24 data, JMAPHOT can use them to model the PSF residuals and the aperture corrections.

We have applied JMAPHOT to the Pismis 24 HRC data. The results for Pismis 24-1NE, 24-1SW, and 24-17 are shown in Table 1. The magnitudes have been corrected for CTE (charge transfer efficiency) and aperture effects and their uncertainties are calculated from the measured S/N plus a contribution from those effects. The aperture correction for F850LP requires a special treatment due to its strong dependence with the spectral energy distribution or SED (Sirianni et al. 2005): we have used a value in accordance with the large extinction of Pismis 24 and we have also added 0.05 mag in quadrature to the F850LP uncertainties to account for this effect. Also, as of the time of this writing there is no low-order flat field calculated for the F220W and F250W filters of ACS HRC. For that reason, we have also added an additional factor of 0.05 mag to the uncertainties for those filters.

Our HRC data consist of 24 individual exposures. Combining the individual JMAPHOT measurements for the separation and position angle of the Pismis 24-1 NE+SW system with their corresponding uncertainties we measured values of 363.86 ± 0.22 mas and 207.816° ± 0.015° east of north, respectively.

2.2. *Spectroscopy*

2.2.1. *Las Campanas*

Spectroscopic observations of Pismis 24-1 NE and SW were obtained with the Inamori Magellan Areal Camera and Spectrograph (IMACS) on the Magellan I (Baade) telescope at Las Campanas Observatory (LCO), on May 9.41 UT, under excellent seeing conditions (0.4″–0.5″), which are characteristic of the Magellan telescopes. We used the f/4 (long) camera with a projected slit width of 2.08 Å to cover the wavelength range 3660–6770 Å at a reciprocal dispersion of 0.38 Å pixel^{-1}. A spectrum of Pismis 24-17 was obtained a few minutes later, with the same instrumentation but somewhat poorer seeing (~0.6″). A He-Ne-Ar comparison spectrum and a flux standard were also observed, as well as the usual series of bias and dome flats. These data were processed at LCO, making use of standard IRAF[6] routines, to yield two-dimensional wavelength- and flux-calibrated images.

[6] IRAF is distributed by the National Optical Astronomy Observatory, which is operated by the Association of Universities for Research in Astronomy, Inc., under cooperative agreement with the National Science Foundation.

Given the separation of only slightly more than 3 pixels between the two Pismis 24-1 components in the IMACS Pismis 24-1 spectra, we used MULTISPEC (Maíz Apellániz 2005) for the extraction. That IDL code is designed to obtain spectra from slitless or long-slit exposures of crowded fields using PSF fitting along the direction perpendicular to the dispersion. The extracted spectra for the three massive stars are shown in Figure 2.

2.2.2. *CASLEO*

Since Lortet et al. (1984) had suggested from observed radial velocity variations that Pismis 24-1 is probably a spectroscopic binary, we acquired high-resolution spectra to test this hypothesis. Spectral images of Pismis 24-1 were obtained with the 2.15 m J. Sahade telescope at Complejo Astronómico El Leoncito (CASLEO) in San Juan, Argentina, during two observing runs: 1998 September and 2000 June. We used the REOSC echelle spectrograph with a TEK 1024 × 1024 pixel^2 detector. The spectral resolving power was $R \sim 15000$. We obtained five exposures covering the wavelength region 3800–6100 Å and three exposures covering 4400–6700 Å. We selected a slit width of 2″ for all of our REOSC spectra, as this was the average seeing during our

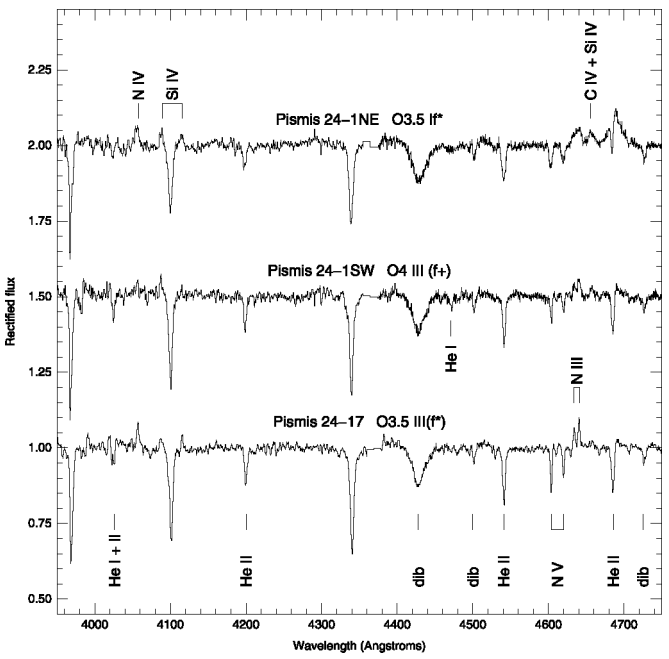

Fig. 2.—Rectified linear intensity spectrograms of Pismis 24-1NE, 24-1SW, and 24-17 obtained with the IMACS-Long Camera of the Baade telescope at Las Campanas Observatory. Each spectrogram has two segments, a violet one and a blue-green one, joined at 4370 Å. The violet segments have been smoothed with 3, 3, and 5 pixel boxes, respectively (*from top to bottom*). The blue-green segment for Pismis 24-17 has been smoothed with a 3 pixel box. Constant values of 0.5 and 1.0 have been added to the Pismis 24-1SW and 24-1NE spectrograms, respectively. The non-DIB lines identified are, in order of increasing wavelength, He I+II λ4026, N IV λ4058, Si IV λλ4089-4116, He II λ4200, He I λ4471, He II λ4541, N V λλ4604-4620, N III λλ4634-4640-4642, Si IV λ4654, C IV λ4658, and He II λ4686, with DIB standing for diffuse interstellar band.

observations. Exposure times for the stellar images ranged between 30 and 45 minutes, resulting in spectra of S/N ~50.

All the spectral images obtained at REOSC were processed and analyzed with standard IRAF routines. We determined radial velocities of the four most conspicuous absorption lines in our spectra, namely the hydrogen absorptions Hγ and Hβ, and the He II absorptions 4541 and 5411 Å, fitting Gaussian profiles within the IRAF routine `splot`. Also, nebular and interstellar lines were measured, and their velocities remained constant within the errors (2–3 km s^{-1}.)

3. THE MOST MASSIVE STARS IN THE CORE OF PISMIS 24

3.1. *Results from Spectroscopy*

The spectral type of Pismis 24-1NE derived from the IMACS data, O3.5 If*, is consistent with that assigned by W02 to the composite observation of the system by Massey et al. (2001). Indeed, that spectrum defined the new type introduced by W02. The key criterion is the comparable intensity of N IV λ4058 and N III $\lambda\lambda$4634-4640-4642 (which stretches the original meaning of "f*" that the N IV is stronger than the N III). Pismis 24-1SW is of later type from both the N IV/N III ratio (the former is weak but still detected) and the weak He I λ4471 absorption line. Indeed, it now appears that the latter feature, as well as the strength of He I+H II λ4026, in the composite data is due to the southwest component. Such is consistent with the nearly identical magnitudes of the two components and the relative morphology of their spectra. The spectral type of Pismis 24-1SW derived from the IMACS observation is O4 III(f+), where the luminosity class follows from the weakened absorption and incipient emission at He II λ4686, and "f+" means that Si IV $\lambda\lambda$4089-4116 are in emission in addition to the N III (which is subsumed in the definition of f*). The spectral type of Pismis 24-17, O3.5 III(f*), is also unchanged from the discussion by W02. The overlap between giant and supergiant absolute visual magnitudes at the earliest spectral types is discussed by W02; in Pismis 24-1 at least one additional component contributes to the relative apparent magnitudes of the resolved pair.

Our REOSC spectra were obtained with worse seeing than the IMACS ones and it is obvious that they contain the combined spectrum of both visual components, Pismis 24-1NE and Pismis 24-1SW, which are less than 0.4″ apart. The absorption lines in our spectra appear to have variable shape, but we did not observe clearly separated component lines in our spectra. We determined the radial velocities of the mean profiles of the absorption lines, with the aim of verifying the previously published radial velocity variations, which most probably would imply that at least one of the visual components of Pismis 24-1 also is a short-period spectroscopic binary. The mean radial velocities of the absorption lines measured in our eight spectra present variations from +20 to −90 km s^{-1} (heliocentric), thus confirming with somewhat larger amplitude the variations published by Lortet et al. (1984). Since we are measuring the lines blended with the visual companion, the actual amplitude of the radial velocity variations may be considerably larger. Our data are too sparse to deduce a value for the orbital period; suffice it to say that it seems to be of only a few days.

Our spectra show the signatures of a turbulent and high-temperature interstellar medium commonly observed in H II regions surrounding very hot stars: namely that the interstellar lines have multiple components, and the presence of nebular absorption of He I λ3888. The main components of the interstellar absorptions of Na I D1 and D2 in our spectra have heliocentric radial velocities of −13 ± 2 and −12 ± 3 km s^{-1}.

Phil Massey and collaborators (2006, private communication) have detected optical variability in the unresolved Pismis 24-1 NE+SW photometry with a peak-to-peak amplitude of 0.07 mag and a period of 2.36088 days. This variability, together with the observed radial velocity variations, is a clear sign that Pismis 24-1 is at least a triple system. Furthermore, the radial velocity of the N IV λ4058 line in the IMACS spectrum coincides with the value derived from our radial velocities obtained from the REOSC spectra at the appropriate orbital phase.[7] Since N IV λ4058 is visible only in the spectrum of Pismis 24-1NE, it must be the spectroscopic binary. We also point out that the fit of the X-ray spectrum of Pismis 24-1 requires a two-temperature plasma model (Wang et al. 2006), which is usually an indication of wind-wind interaction in a relatively close binary. The results here point toward Pismis 24-1NE as the source of the hard X-ray component.

3.2. *Results from Photometry*

The results in Table 1 show that Pismis 24-1NE is brighter than 24-1SW in the optical/NUV by ~0.1 mag, with nearly identical colors. Given their very similar spectral type and location, this is as expected: both stars have almost the same intrinsic colors and their light is affected by the same amount and type of dust. The most significant difference is in F550M − F658N [V − (Hα+continuum)], where Pismis 24-1NE is redder by 0.069 ± 0.025 mag. This is also expected, since 24-1NE is a supergiant and has a stronger Hα emission (this effect is also seen in our LCO spectra). Pismis 24-1NE is brighter than 24-17 by 0.924 ± 0.016 mag in F330W, but the latter is slightly redder than either of the 24-1 components; hence, the difference at F850LP is reduced to 0.651 ± 0.007 mag.[8] The likely source for the color differences is that the light from Pismis 24-17 is more extincted than that from 24-1.

We have processed the Pismis 24-1NE, 24-1SW, and 24-17 photometry with CHORIZOS (Maíz Apellániz 2004), a Bayesian code that compares observed magnitudes with SED families and calculates the likelihood distribution. The current version of the code includes the most recent calibration for optical and NIR photometric zero points (Maíz Apellániz 2007b). For each of the stars we have fixed the values of the temperature and gravity derived from their spectral types and the calibration of Martins et al. (2005) and we have left R_{5495} and $E(4405-5495)$, the monochromatic equivalents of R_V and $E(B-V)$, as free parameters using the extinction law family of Cardelli et al. (1989). For each star we have used as input SEDs both the CMFGEN grid calculated by Martins et al. (2005) and the TLUSTY OSTAR2002 grid of Lanz & Hubeny (2003); however, after running CHORIZOS with the two SED families, we could find no significant differences between them (not surprising, considering that they both have very similar intrinsic colors for a given temperature and gravity). Therefore, here we report only on the results for the CMFGEN case. Both Pismis 24-1 and Pismis 24-17 have 2MASS JHK_s photometry, although Pismis 24-1 is unresolved. Given the increased accuracy of the extinction corrections when NIR photometry is included in CHORIZOS, we have done two different runs for each object: one with F330W+F435W+F550M+F850LP and another one with those same filters plus JHK_s. Given that Pismis 24-1 is unresolved in 2MASS, for its run with 2MASS we merged the HRC photometry for 24-1NE and 24-1SW.

[7] Note, however, that we have insufficient points to determine a full velocity curve, which we will obtain in the future.

[8] Most of the uncertainty for F850LP is due to the aperture correction, so it should not be applied to magnitude differences within the same filter.

TABLE 2
CHORIZOS RESULTS

Object	2MASS	A_{F550M}	R_{5495}	M_V	$(m - A + BC)_{F550M}$	χ^2_{min}	dof
Pismis 24-1NE	No	5.54 ± 0.10	2.87 ± 0.05	−6.41 ± 0.17	1.71 ± 0.10	9.1	1
Pismis 24-1SW	No	5.52 ± 0.10	2.87 ± 0.05	−6.28 ± 0.17	1.73 ± 0.10	7.0	1
Pismis 24-17	No	5.91 ± 0.11	2.94 ± 0.05	−6.01 ± 0.17	1.91 ± 0.10	4.6	1
Pismis 24-1	Yes	5.87 ± 0.02	3.01 ± 0.01	−7.50 ± 0.14	0.57 ± 0.02	40.4	4
Pismis 24-17	Yes	6.34 ± 0.02	3.11 ± 0.02	−6.50 ± 0.14	1.42 ± 0.02	26.1	4

The results of the five CHORIZOS runs are shown in Table 2: the total extinction in F550M, the extinction law, the absolute visual magnitude [adopting from Massey et al. (2001) a distance modulus of $(m - M)_0 = 12.03 \pm 0.14$], the apparent bolometric magnitude (i.e., the observed F550M magnitude with its extinction and bolometric corrections), the minimum χ^2, and the degrees of freedom of the fit. In all cases, a single well-defined solution is present in the likelihood R_{5495} versus $E(4405 - 5495)$ plots. The mode SED is shown in Figure 3 for Pismis 24-1NE (without 2MASS) and for Pismis 24-1 (with 2MASS).

1. All the runs yield extinctions in F550M close to 6 mag and R_{5495} values close to 3.0. The latter are significantly lower than the results found by Bohigas et al. (2004).
2. Pismis 24-17 is more extinguished than Pismis 24-1 by ≈0.4 mag, which is consistent with the Bohigas et al. (2004) results, although our values are lower overall.
3. The inclusion of the 2MASS data introduces significant changes in the results, increasing the measured F550M extinction by ≈0.4 mag and R_{5495} by ≈0.15.
4. The minimum χ^2 values are too high. We attribute this to the Cardelli et al. (1989) extinction law, which was derived with an older photometric calibration (see Maíz Apellániz 2006) and using only moderately extinguished stars. It also uses a rather unphysical seventh-degree polynomial in the optical region, which is responsible for the long-period oscillations in wavelength visible in the reddened SEDs in Figure 3, an effect that is unlikely to be real and that artificially increases the χ^2 values.

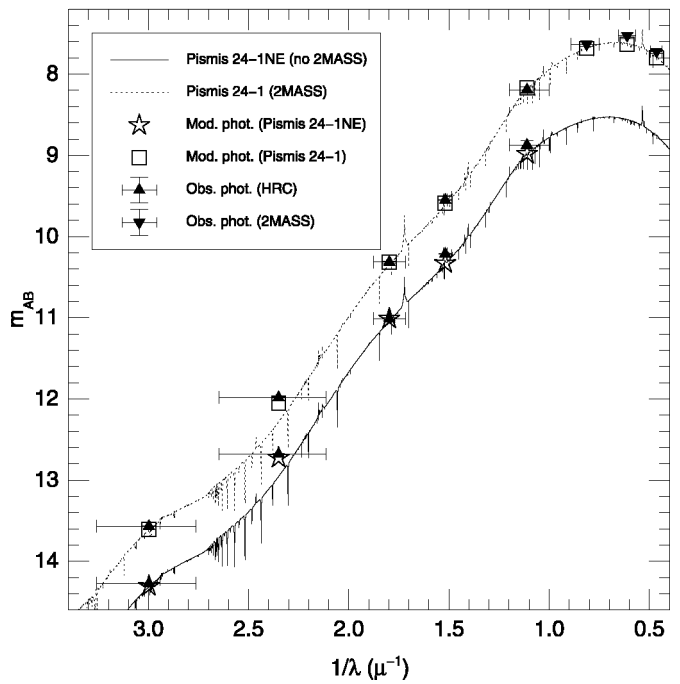

FIG. 3.—Mode SEDs and synthetic photometry for two of the CHORIZOS runs. The observed photometry is also shown, with the horizontal error bars marking the approximate extent of each of the seven filters (from left to right, HRC F330W, F435W, F550M, F658N, and F850LP; 2MASS J, H, and K_s) and the vertical error bars (small in all cases) for the photometric uncertainties. The F658N (Hα) filter is not included in the CHORIZOS runs but is shown here for comparison; note how the emission excess is larger for Pismis 24-1NE than for Pismis 24-1.

We have used the CHORIZOS results to derive new evolutionary zero-age masses for the three objects in our sample. The evolutionary tracks have been obtained from Lejeune & Schaerer (2001). Additional uncertainties of 0.1 mag have been added in quadrature to the bolometric magnitudes to take into account the problems with the extinction correction and the (small) uncertainty in the effective temperatures. The 2MASS information was included in the calculations because its presence significantly reduces the systematic errors introduced by the seventh-degree polynomial used for the extinction law in the optical (in any case, it is always good practice to add NIR data to optical photometry when analyzing objects with moderate or high extinction). We obtain nearly identical values for the three objects: 97 ± 10 $M_\odot$ (Pismis 24-1NE), 96 ± 10 $M_\odot$ (Pismis 24-1SW), and 92 ± 9 $M_\odot$ (Pismis 24-17). The real mass for the unresolved components in Pismis 24-1NE must be, of course, smaller: if the luminosity is equally split and the temperature is the same for both, the resulting values are of the order of 64 $M_\odot$ for each.

As a test, we can also compute the mass of Pismis 24-1 as if it were a single star (i.e., the W02 hypothesis) and we obtain[9] 155 ± 19 $M_\odot$. This value is much lower than those obtained by W02 (210 or 291 $M_\odot$). Given that our value for M_V is very similar to theirs, the difference must arise from the different temperature scales used (Martins et al. [2005], derived from line-blanketed models, versus Vacca et al. [1996]). The reduction in temperature for a given spectral type motivated by the change moves the star in an H-R diagram toward the lower right (the vertical effect is due to the smaller bolometric correction). Such a displacement is almost perpendicular to the evolutionary tracks for O stars that are just evolving off the main sequence and, thus, is a very effective way of reducing the mass estimate.

What else could be affecting the masses? Even though Pismis 24 suffers moderate extinction ($A_V \approx 6$ mag), future improvements in this respect are likely not to be too large, since our analysis includes multiband optical and NIR data simultaneously and A_K is only ≈0.6 mag. Also, our *HST* optical photometry is compatible with modern ground-based results and Tycho did not detect photometric variability, so the possibility of undetected changes (other than those caused by the known eclipses) seems unlikely. Finally, the distance calculated by Massey et al. (2001) could be wrong; we plan to test that possibility in the near future by making use of our additional *HST* data.

[9] Note that the evolutionary track with the highest mass is 120 $M_\odot$, so we are forced to extrapolate, a procedure that should introduce additional uncertainties.

4. CONCLUSIONS

We have presented *HST* and ground-based data that clearly resolve Pismis 24-1 into two objects separated by 363.86 mas and that indicate the existence of at least a third unresolved component in Pismis 24-1NE. We have also derived zero-age evolutionary masses for the three most massive objects at the core of Pismis 24-1, with values of 92–97 $M_{\odot}$, one of them corresponding to the unresolved system Pismis 24-1NE. These values are very large, making the cores of Pismis 24-1 and Trumpler 14 (Nelan et al. 2004) the two locations within 3 kpc of the Sun with the highest density of very massive stars. However, these masses are not above what it is currently thought to be the stellar upper mass limit.

After this manuscript was submitted, Virpi Niemela, one of the authors, passed away. The rest of the authors want to dedicate this article to her memory. She was the first one of us to study Pismis 24-1 and also the first one to suspect its multiplicity. But, more importantly, she was a wonderful human being to whom a generation of astronomers is indebted for her insight and her warmth.

We would like to thank Phil Massey and his team of collaborators for letting us know about the optical photometric variability prior to publication and David Osip and Mark Phillips for kindly allowing us to use IMACS during part of an engineering night at the Baade telescope. We also acknowledge the useful comments made by an anonymous referee. Support for this work was provided by (1) the Spanish Government through grant AYA2004-08260-C03; (2) NASA through grant GO-10602 from the Space Telescope Science Institute, which is operated by the Association of Universities for Research in Astronomy Inc., under NASA contract NAS 5-26555; and (3) IALP-CONICET, Argentina.

REFERENCES

Anderson, J., & King, I. R. 2004, ACS Instrument Science Report 2004-15 (Baltimore: STScI)
Bohigas, J., Tapia, M., Roth, M., & Ruiz, M. T. 2004, AJ, 127, 2826
Bonanos, A. Z., et al. 2004, ApJ, 611, L33
Cardelli, J. A., Clayton, G. C., & Mathis, J. S. 1989, ApJ, 345, 245
Figer, D. F. 2005, Nature, 434, 192
Koen, C. 2006, MNRAS, 365, 590
Lanz, T., & Hubeny, I. 2003, ApJS, 146, 417
Lejeune, T., & Schaerer, D. 2001, A&A, 366, 538
Lortet, M. C., Testor, G., & Niemela, V. 1984, A&A, 140, 24
Maíz Apellániz, J. 2004, PASP, 116, 859
———. 2005, STIS Instrument Science Report 2005-02 (Baltimore: STScI)
———. 2006, AJ, 131, 1184
———. 2007a, ACS Instrument Science Report, in press (Baltimore: STScI)
———. 2007b, in ASP Conf. Ser. 364, The Future of Photometric, Spectrophotometric, and Polarimetric Standardization, ed. C. Sterken (San Francisco: ASP), in press (astro-ph/0609430)
Maíz Apellániz, J., Walborn, N. R., Galué, H. Á., & Wei, L. H. 2004, ApJS, 151, 103
Martins, F., Schaerer, D., & Hillier, D. J. 2005, A&A, 436, 1049
Mason, B. D., Gies, D. R., Hartkopf, W. I., Bagnuolo, W. G., Brummelaar, T. T., & McAlister, H. A. 1998, AJ, 115, 821
Massey, P., DeGioia-Eastwood, K., & Waterhouse, E. 2001, AJ, 121, 1050
Morrell, N. I., Walborn, N. R., & Arias, J. I. 2005, PASP, 117, 699
Nelan, E. P., Walborn, N. R., Wallace, D. J., Moffat, A. F. J., Makidon, R. B., Gies, D. R., & Panagia, N. 2004, AJ, 128, 323
Niemela, V., & Gamen, R. 2004, NewA Rev., 48, 727
Oey, M. S., & Clarke, C. J. 2005, ApJ, 620, L43
Rauw, G., et al. 2004, A&A, 420, L9
Schaller, G., Schaerer, D., Meynet, G., & Maeder, A. 1992, A&AS, 96, 269
Sirianni, M., et al. 2005, PASP, 117, 1049
Vacca, W. D., Garmany, C. D., & Shull, J. M. 1996, ApJ, 460, 914
Vijapurkar, J., & Drilling, J. S. 1993, ApJS, 89, 293
Walborn, N. R. 1971, ApJ, 167, L31
Walborn, N. R., Drissen, L., Parker, J. W., Saha, A., MacKenty, J. W., & White, R. L. 1999, AJ, 118, 1684
Walborn, N. R., et al. 2002, AJ, 123, 2754
Wang, J., Townsley, L. K., Feigelson, E. D., Getman, K. V., Broos, P. S., Garmine, G. P., & Tsujimoto, M. 2006, preprint (astro-ph/0609304)
Weidner, C., & Kroupa, P. 2004, MNRAS, 348, 187